CD38 assigns physiological function to soluble uric acid

Shijie Wen[1], Hiroshi Arakawa[1], Shigeru Yokoyama[2,3], Yoshiyuki Shirasaka[1], Haruhiro Higashida[2], Ikumi Tamai[1,4*]

[1]Faculty of Pharmaceutical Sciences, Institute of Medical, Pharmaceutical and Health Sciences, Kanazawa University, Kanazawa, Japan

[2]Research Center for Child Mental Development, Kanazawa University, Kanazawa, Japan

[3]Division of Socio-Cognitive-Neuroscience, United Graduate School of Child Development, Osaka University, Kanazawa University, Hamamatsu University School of Medicine, Chiba University and University of Fukui, Kanazawa, Japan.

[4]Lead contact

[*]Correspondence: tamai@p.kanazawa-u.ac.jp (I.T.)

Summary

Excessive elevation of soluble uric acid (sUA) is associated with the risk of various diseases. However, evolutionary biology implies that sUA has unassigned physiological functions and targets. Here, we demonstrate that sUA directly inhibits the hydrolase and cyclase activities of CD38, a major enzyme responsible for NAD^+ degradation, via a reversible non-competitive mechanism, thereby increasing NAD^+ availability. CD38 inhibition is restricted to sUA in purine metabolic pathways. A structural comparison using analogs shows that 1,3-dihydroimidazol-2-one is the main functional group for CD38 inhibition, while the adjacent uracil-like heterocycles are also essential. Moreover, mild and short-term elevation of plasma sUA prevents crude lipopolysaccharide (cLPS)-induced systemic inflammation and monosodium urate (MSU) crystal-induced peritonitis by interacting with CD38. Taken together, this study reveals that sUA functions as an endogenous inhibitor of CD38 to physiologically limit NAD^+ degradation and innate immunity.

Keywords: uric acid, MSU crystals, uricase, CD38, inflammation, innate immunity, immunometabolism, NAD^+, hyperuricemia, hypouricemia

Introduction

The evolutionary loss of uricase activity in humans and certain primates completely blocks the degradation of soluble uric acid (sUA), leading to higher sUA levels than in other mammals[1,2]. sUA is synthesized in several tissues and primarily excreted via the kidney. Additionally, we first identified its extra-renal elimination mediated by intestinal breast cancer resistance protein (BCRP) in 2012[3]. As the final metabolite of purines, sUA is strictly maintained in humans owing to renal reabsorption, implying its key role in physiology. For decades, sUA has been proposed to critically maintain blood pressure[4] and to function as the most abundant antioxidant[5] in humans. However, excessive elevation of sUA may promote the precipitation of monosodium urate (MSU) crystals to cause diseases such as gout[6] and kidney stone disease[7]. On the basis of the

NLRP3 inflammasome activation by MSU crystals[8], it has been suggested that chemical phase transition is essential for sUA as a danger signal to trigger immune responses[9-13]. Conversely, sUA decline in uricase-transgenic mice increases mortality and promotes sterile inflammation[14], whereas crystal-free hyperuricemia suppresses neutrophil recruitment and monocyte activation[12,13], supporting the physiologically essential role of sUA in host immunity and metabolism. In fact, UMP synthase was identified as a direct target of sUA in 2017[15]; however, it does not fully explain the physiological functions of sUA, suggesting other unknown physiological targets.

To further explore the physiological functions of sUA and identify the potential targets, we searched for sUA-binding proteins at first. In the preliminary screening, we employed magnetic bead-conjugated 8-oxyguanine (8-OG, an sUA analog) and proteomic analysis to capture several potential candidates, including CD38, which was finally identified as a physiological target for sUA in this study.

CD38 is a multifunctional enzyme and receptor that plays a pivotal role in inflammation, aging, cancer, and metabolic disorders[16]. Its cyclase catalyzes the synthesis of cyclic ADP-ribose (cADPR) from NAD^+ to regulate calcium mobilization[17,18], which is crucial for social behavior[19] and neutrophil recruitment[20]. CD38 mainly functions as a hydrolase to degrade NAD^+[21], the increased hydrolase activity during aging drives NAD^+ decline, resulting in metabolic disorders[22-24]. In addition to enzymatic activity, CD38 may also serve as a receptor for adhesion molecules such as CD31 to regulate cell migration and homing[25,26]. Inhibition or deficiency of CD38 suppresses inflammation[27], aging-related dysfunction[22,23], and the progression of neurodegenerative diseases such as Alzheimer's disease[28] and multiple sclerosis[29]. Clinical observations[30,31] and experimental evidence[12,32-34] suggest similar protective effects of sUA. However, the role of CD38 in sUA physiology remains poorly understood.

Here, we reveal that sUA directly inhibits CD38 and consequently limits NAD^+ degradation and innate immunity, which first defines the physiological functions of sUA via CD38. Moreover, we confirm the unique effect of sUA on CD38 in purine

metabolic pathways and identify a structural feature for pharmacological inhibition of CD38.

Results

Soluble uric acid is a non-competitive and reversible inhibitor for CD38

To reveal the target-based physiological functions of sUA, we first captured CD38 as a binding protein of 8-OG, as evidenced by enzyme inhibition (Figure 1A), which raised our interest in exploring the interaction between sUA and CD38. As expected, sUA directly inhibited the hydrolase and cyclase activities of human (Figures 1B, 1C, and S1B) and murine CD38 (Figure 1F) as a non-competitive inhibitor (Figures 1D, 1E, and S1A) with micromolar K_i (57.14-93.31 μM), suggesting its binding to the allosteric sites of CD38. sUA showed comparable inhibitory effects on hydrolase and cyclase, as indicated by similar K_i. The physiological levels of sUA in humans (about 120-420 μM[35,36]) and several mouse tissues (Figure S1K) were higher than its K_i, indicating that CD38 is physiologically inhibited by sUA. The inhibitory effects were reversible (Figures 1G, 1H, S1C, and S1D), suggesting that sUA dynamically modulates CD38 activity. Interference from endogenous sUA was negligible when using tissues as an enzyme source, because the concentrations in the final reaction buffer were below 1 μM (Figure S1J).

CD38 inhibition is restricted to soluble uric acid in purine metabolic pathways

Although the structure of sUA is similar to that of other purines, we confirmed its unique effect on CD38 in the major metabolic pathways of purines (Figure 2C). sUA precursors (adenosine, guanosine, inosine, hypoxanthine and xanthine) and the metabolite (allantoin) hardly inhibited the hydrolase and cyclase activities of human (Figures 2A, 2B, and S1E) and murine (Figures S1F and S1G) CD38. The tested purine concentrations were higher than their physiological levels[37-39]. Thus, CD38 inhibition is restricted to sUA, suggesting a specific functional group in sUA.

To identify the functional group for CD38 inhibition, we tested additional xanthine

analogs (oxypurinol and caffeine) and sUA analogs (1-methyluric acid (1-MU) and 1,3-dimethyluric acid (1,3-DMU)). Only the sUA analogues inhibited CD38 activity (Figure 2D). A structural comparison (Figure 2F) indicated that 1,3-dihydroimidazol-2-one is the functional group, as all other purines lacking this group failed to inhibit CD38 activity. However, the ring-opening of the uracil group after sUA conversion to allantoin abrogated this inhibitory potential. Uracil or 1,3-dihydroimidazol-2-one (Figures 2E, S1H, and S1I) alone did not affect CD38 activity. Therefore, the adjacent uracil-like heterocycles are also essential for CD38 inhibition.

Soluble uric acid increases NAD^+ availability by inhibiting CD38

CD38 is a key enzyme in the degradation of NAD^+ and its precursor, nicotinamide mononucleotide (NMN)[24], we next explored the effect of sUA on NAD^+ availability. sUA was found to increase intracellular NAD^+ in A549 and THP-1 cells (Figures S3A and S3B), then we focused on the *in vivo* regulatory effect of sUA via CD38. We constructed mild and short-term "hyperuricemia" model by gavage of inosine and oxonic acid (OA, uricase inhibitor) in mice with "natural hypouricemia," as validated by plasma sUA (Figures 3D and S2C). The plasma sUA levels (around 120 μM) in our models were close to the minimal physiological concentration in humans but higher than its K_i, which enabled us to evaluate the physiological inhibition of CD38 by sUA. OA (nanomolar K_i for uricase[40]) was a weak inhibitor of CD38 with millimolar IC_{50} (Figures S1L and S1M), whereas it seemed unlikely to affect CD38 activity in our models because of the incomplete inhibition of uricase, as evidenced by plasma sUA (Figure S1N). Although OA alone failed to increase sUA levels, we used it as the background for metabolic studies in mice to exclude potential interference.

One-day or 3-day mild-elevation of plasma sUA slightly but significantly increased whole blood NAD^+ levels in wild-type (WT) mice but not in CD38 knockout (KO) mice (Figures 3A, 3D, S2C, and S2D), similar results were also observed under inflammatory conditions (Figures S3H, S3I, S3P, and S3Q). This indicates that CD38 is, at least in part, involved in the suppressive effect of sUA on NAD^+ degradation. The suppression

of NAD^+ degradation by the sUA-CD38 interaction was validated by decreased cADPR production under inflammatory conditions (Figure S3K) but not under non-inflammatory conditions (Figures 3C and S2F), possibly because of physiological compensation via other cADPR synthases. However, sUA showed a minor effect on NMN levels *in vivo* (Figures 3B, S2E, S3J, and S3R), likely due to the rapid conversion of NMN to NAD^+[41]. Notably, WT and CD38 KO mice showed similar NAD^+ baselines in whole blood, suggesting that the metabolic background has been reprogrammed in CD38 KO mice; for instance, additional NAD^+ may fuel sirtuins with higher activity[22]. Moreover, sUA release *in vivo* showed that both plasma sUA and whole blood NAD^+ gradually returned to their initial levels (Figures 3E-3L), which confirmed the reversible regulation of NAD^+ availability by sUA and excluded potential interference from epigenetic regulation of other bioconversion pathways of NAD^+. Metabolic assays using recombinant hCD38 further verified that increased NAD^+ availability is mediated by direct CD38-sUA interaction (Figures 3M and 3N).

In contrast, the tissue levels of sUA, NAD^+, and NMN were hardly increased in 1-day and 3-day models (Figures S2A and S2B), probably because the tissue uptake of sUA was physiologically saturated before treatment. The NAD^+ levels in the brain and heart appeared to be elevated in 7-day model (Figures S2G-S2I). Thus, the sUA-CD38 interaction in the circulation may indirectly increase tissue NAD^+ availability. Our models did not show pro-inflammatory potential (Figure S4Q), and we did not prolong the treatment time because long-term administration of OA might induce kidney injury with concomitant inflammation.

Considering the rapid conversion of NMN to NAD^+ *in vivo*, we assessed the effect of sUA on extracellular NMN degradation *in vitro*. sUA directly inhibited NMN degradation by recombinant hCD38 (Figure S3C). Whereas sUA or other CD38 inhibitors failed to boost intracellular NAD^+ in primed WT bone marrow-derived macrophages (BMDMs) treated with NMN (Figure S3D). This is likely because another NAD^+-consuming enzyme, PARP1, is activated[42] and the expression level of NMN transporter may be very low in BMDMs[24]. Importantly, sUA increased extracellular

NMN availability in WT BMDMs (Figure S3E) but not in CD38 KO BMDMs (Figure S3F). The addition of recombinant hCD38 restored the suppressive effect of sUA on extracellular NMN degradation in CD38 KO BMDMs (Figure S3G). Accordingly, sUA may increase NAD^+ availability by inhibiting CD38-medaited NMN degradation.

Soluble uric acid limits innate immunity via interacting with CD38

NAD^+ is crucial for sirtuins to limit the NLRP3 inflammasome activation[43], and cADPR may regulate calcium signaling to promote cytokine production[44,45]. Therefore, CD38 may play a key role in inflammation via NAD^+ metabolism. We confirmed the role of CD38 in NLRP3 inflammasome activation. CD38 KO reduced IL-1β release driven by inflammasome activators and the fungal component zymosan in primed BMDMs (Figure S4A). Pre-incubation with sUA moderately suppressed inflammasome activation in primed THP-1 cells (Figure S4H) but not in primed WT BMDMs (Figure S4B). In fact, sUA uptake was very low in primed WT BMDMs (Figure S4D), suggesting that intracellular sUA plays a crucial role in the regulation of inflammasome activation *in vitro*. However, this does not exclude the effect of extracellular sUA on inflammation *in vivo*, as it may limit extracellular NMN degradation via CD38 to increase NAD^+ levels *in vivo*, and consequently suppress inflammasome activation via sirtuin signaling[43]. Additionally, sUA did not induce IL-1β release in primed WT BMDMs and THP-1 cells (Figures S4C and S4H). Our results argue against the pro-inflammatory potential of sUA[46] that has been challenged by the improper preparation of aqueous solution in basic studies[11,12]. In fact, we confirmed that long-term storage at 4 °C also promoted crystal precipitation in the stock solutions of sUA (Figure S4R).

Owing to the limitations of *in vitro* models, we stimulated WT and CD38 KO mice with crude lipopolysaccharide (cLPS) after 1-day elevation of plasma sUA to assess the role of CD38 in the immunosuppression of sUA. To exclude any potential effects of OA, we used it as the background in mice. Plasma sUA elevation suppressed cLPS-induced production of IL-1β and IL-18 without affecting inflammasome-independent

TNF-α levels in the serum (Figures 4A-4C), while these effects were abrogated in CD38 KO mice, demonstrating that sUA suppresses cLPS-induced systemic inflammation via CD38. Mechanistically, the immunosuppression we observed may be partially mediated by increased NAD^+ levels and decreased cADPR production in whole blood after sUA-CD38 interaction (Figures S3I and S3K). sUA hardly limited high-dose cLPS-induced systemic inflammation (Figures S4I-S4K), although plasma sUA and whole blood NAD^+ levels were increased (Figures S3P and S3Q). In addition, high-dose cLPS, with or without plasma sUA elevation, did not affect cADPR levels (Figure S3S), suggesting some CD38-independent inflammatory mechanisms.

Recently, sUA has been reported to inhibit neutrophil migration rapidly[13], suggesting that some biological targets directly mediate sUA immunosuppression[47]. CD38 is essential for neutrophil recruitment[20], we therefore investigated the effect of sUA on MSU crystal-induced peritonitis via CD38. One-day elevation of plasma sUA inhibited the recruitment of viable cells and neutrophils and reduced the production of IL-1β and IL-6 in WT mice but not in CD38 KO mice (Figures 4D, 4E, 4G, and 4H), which verified the involvement of CD38 in the suppression of innate immunity by sUA. CXCL1 production (Figure 4F) was unaffected by sUA, indicating that the sUA-CD38 interaction may inhibit circulating immune cells in response to chemokines. Moreover, sUA may interfere with the CD38-CD31 interaction to suppress immune cell migration. Intriguingly, intact IL-8 signaling has been reported in CD38 KO mice[20], and sUA at high concentration (595 μM) inhibits neutrophils in response to IL-8[13]. Whereas we did not observe decreased neutrophils recruitment by sUA in CD38 KO mice, it is likely because plasma sUA levels in our models are insufficient to affect IL-8 signaling. In addition, we cannot exclude the possibility that CD38 is essential for the inhibitory effects of sUA on IL-8 signaling and β2-integrin, which requires further investigation in the future.

Inosine may also exhibit anti-inflammatory effects via adenosine receptors[48]. Scott GS, et al. reported that after oral administration, inosine concentrations slightly increase and then rapidly return to the initial levels in mice within 2 h[34]. We stimulated the mice

with cLPS or MSU crystals 2 h after the last treatment, suggesting that the contribution of inosine is negligible. To verify this, we evaluated the effects of inosine or OA on inflammation *in vivo*. Both hardly affected cLPS-induced systemic inflammation (Figures S4E-S4G) and MSU crystal-induced peritonitis (Figures S4L-S4P), as well as sUA levels and NAD^+ metabolism under inflammatory conditions (Figures S3L-S3O). Thus, we conclude that CD38 mediates, at least in part, the suppressive effects of sUA on innate immunity.

Discussion

In humans and certain primates, the evolutionary loss of uricase activity appears to be caused by various factors that are difficult to pinpoint and tease apart, and its advantages and disadvantages remain elusive[49,50]. Dominant reabsorption (approximately 90%) of filtered sUA in the kidney implies that humans have to keep sUA at certain levels to maintain its potential physiological function, rather than completely eliminating it as harmful waste. Our study identifies sUA as an endogenous inhibitor of CD38, and reveals its suppressive effects on NAD^+ degradation and innate immunity via CD38. The functions of sUA assigned by CD38 may promote understanding of sUA physiology and challenge traditional opinions on its pathophysiology.

NAD^+ decline contributes to aging-related dysfunction and multiple diseases, including hearing loss, obesity, diabetes, kidney diseases, and cardiovascular diseases, in murine models[21] and possibly even in humans[51]. Accordingly, NAD^+ boosting by CD38 inhibitors has been proposed as a promising therapeutic strategy[16,21,52]. We unveil a structural feature for CD38 inhibition based on sUA analogs, which may promote the development of new inhibitors with ideal pharmacokinetic properties because sUA is rarely metabolized but is well distributed in humans, although chemical modification may be required to improve inhibitory efficiency and specificity. Importantly, our results suggest that sUA at physiological concentration can limit CD38 activity and consequently maintain NAD^+ levels, which may prevent related diseases and delay

248 senescence. Thus, sUA is physiologically essential for humans and certain primates,
249 and hypouricemia may negatively influence host metabolism. However, we cannot
250 exclude the possibility that long-term and crystal-free hyperuricemia (> 420 μM) in
251 humans may overly modulate additional unknown targets, especially in CD38 negative
252 cells, thereby partially covering the CD38-mediated physiological functions of sUA.

253 Given the physiological functions of sUA, the risks and benefits of urate-lowering
254 therapy should be prudently weighed up in the clinical setting. Rapid urate lowering in
255 the initiation of therapy even increases the risk of gout flares in patients[53]. Similar to
256 itaconate, an inhibitor of NLRP3 inflammasome[54], sUA production increases in
257 activated macrophages[55]; thus, it may function as an endogenous regulator of
258 inflammasomes via CD38 to avoid excess inflammation. Previously, we demonstrated
259 that MSU crystals upregulate CD38 expression to promote gouty inflammation in
260 primed macrophages[56]. Conversely, this study reveals that sUA physiologically limits
261 gouty inflammation via CD38 inhibition, although the mechanisms by which CD38
262 regulates host immunity are not fully understood. Therefore, CD38 mediates the
263 opposite effects of sUA and its crystals on innate immunity. Intracellular and/or
264 extracellular crystals should be excluded when evaluating the pathological potential of
265 sUA. Additionally, our findings imply that sUA levels control CD38 activity to regulate
266 innate immunity. The balance between sUA and the remaining crystals may
267 dynamically remodel the immunity of gout patients during urate-lowering therapy
268 (Fig.S4S). This may explain why moderate but not rapid urate-lowering is
269 recommended to reduce the initial risk of gout flares in patients[57,58].

270 CD38 inhibition also supports the role of sUA in neurobiology. As mentioned
271 previously, CD38 plays a central role in some neurodegenerative diseases, and
272 numerous clinical observations have indicated the potential neuroprotective effects of
273 sUA. Thus, sUA may directly cross the blood-brain barrier under pathological
274 conditions and subsequently inhibit CD38 activity in specific regions of the brain to
275 limit neuroinflammation. Additionally, CD38 is crucial for neuropeptide release to
276 regulate social behavior[19]. The delivery of circulating sUA to the brain is limited under

physiological conditions; however, further studies are required to assess the influence of peripheral sUA-CD38 interaction on social behavior.

Previously, a physiological medium containing sUA was shown to inhibit UMP synthase and reduce the chemotherapeutic sensitivity of cancer cells[15]. Based on our findings, sUA appears to broadly regulate cellular metabolism via different targets. Although we identify a direct sUA-CD38 interaction, more extensive effects on host metabolism and adaptive immunity are still unknown and of potential interest for future studies. Importantly, the physiological functions of sUA should draw more attention in clinical practice, and targeting sUA may overcome some immunological or metabolic disorders.

Limitations of Study

The commercial recombinant hCD38 without a transmembrane region was used in this study, we cannot exclude the potential interaction between sUA and the transmembrane region of CD38, although we obtained comparable K_i using crude enzymes containing full-length CD38. The crystal structure of the active full-length CD38-sUA complex should be captured using cryo-electron microscopy to elucidate the inhibitory mechanisms. Moreover, our *in vivo* models hardly increased tissue sUA levels, and further studies are required to confirm its physiological function in different tissues by constructing uricase-transgenic mice from WT or CD38 KO strains.

Acknowledgments

This study was supported by Grant-in-Aid for Scientific Research (B) [21H02641] (I.T.) from the Japan Society for the Promotion of Science (JSPS) and Research Grant 2022 from Gout and Uric Acid Foundation of Japan (I.T.). S.W. was funded by the Japanese Government (Monbukagakusho: MEXT) Scholarship Program and Kanazawa University. The authors thank Dr. Zheng Jing, Ms. Aimi Taniguchi, Mr. Kazuki Himi, and Mr. Kazuki Fujita for providing assistance.

Author contributions

S.W and I.T. designed the study. S.W. performed experiments, analyzed the data, and wrote the manuscript. H.A. provided support in the whole project. S.W., H.A., H.H, and I.T. edited the manuscript, all the authors read and approved the manuscript. S.Y., Y.S., and H.H. provided animals, and/or a part of materials and instruments. H.A., S.Y., and H.H. assisted with experimental design. I.T. supervised the whole project.

Declaration of interests

The authors declare no competing interests.

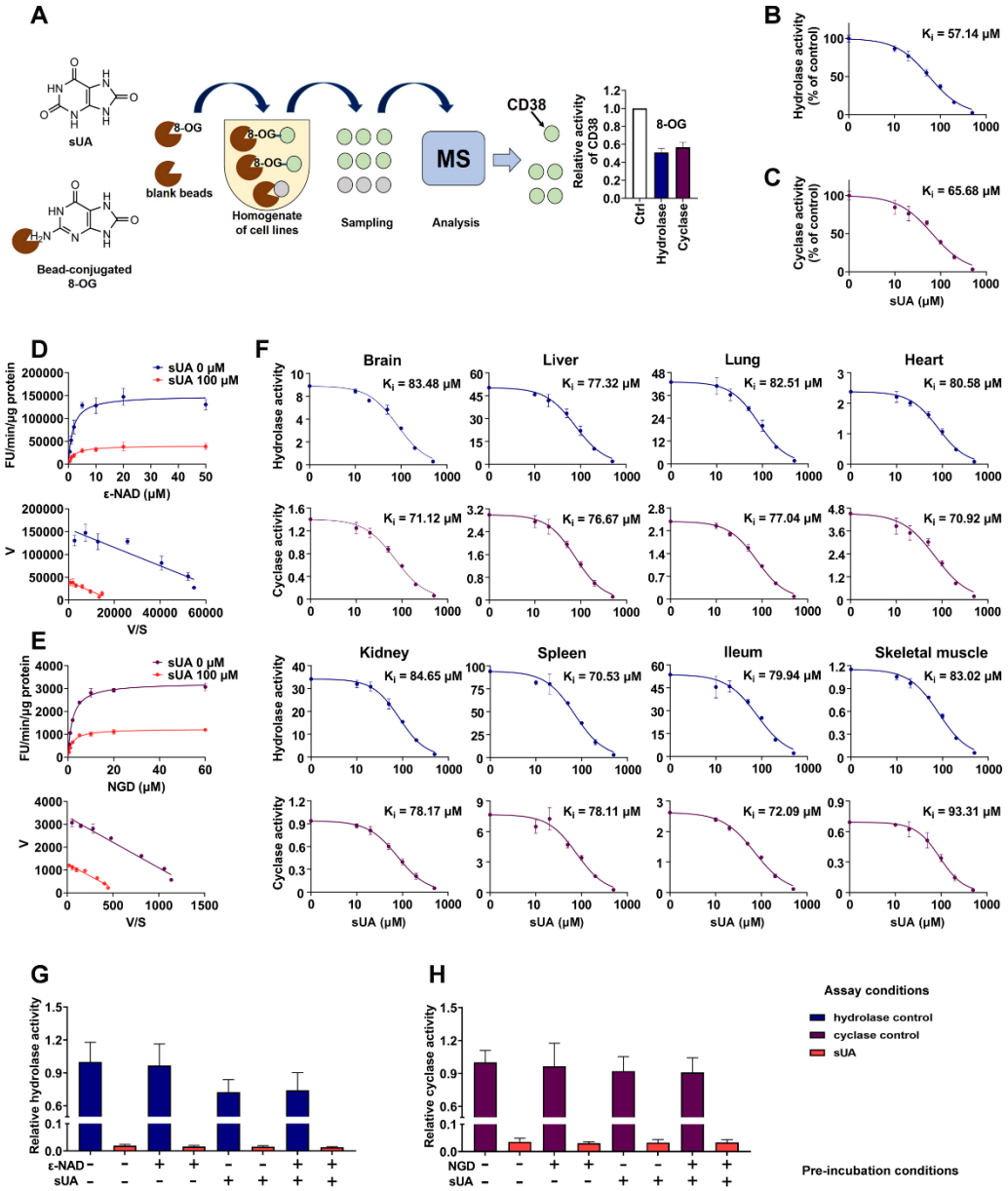

Figure 1. Identification of sUA as an endogenous inhibitor for CD38

(A) Preliminary screening of 8-OG binding proteins by mass spectrum (MS)-based proteomics, and effect of 8-OG (50 μM) on CD38 activity. (n = 3 experiments)

(B and C) Hydrolase and cyclase activities of recombinant hCD38 in the presence of sUA, using nicotinamide 1, N^6-ethenoadenine dinucleotide (ε-NAD^+), and nicotinamide guanine dinucleotide (NGD) as substrates, respectively. (n = 3 experiments)

(D and E) Effect of different substrate concentrations on sUA inhibition of recombinant hCD38 hydrolase (D) and cyclase (E) activities. (n = 3 experiments)

326 (F) Effect of different sUA concentrations on hydrolase and cyclase activities
327 (FU/min/μg protein) in tissues from 8- to 12-week-old WT mice. (n = 3 experiments)
328 (G and H) Reversibility of inhibition of recombinant hCD38 hydrolase (G) and cyclase
329 (H) activities by sUA. After 30-min pre-incubation as indicated, samples were diluted
330 100-fold in reaction buffer with or without 500 μM sUA for enzyme assay. (n = 3-5
331 experiments)
332 Data are mean ± s.d.
333
334

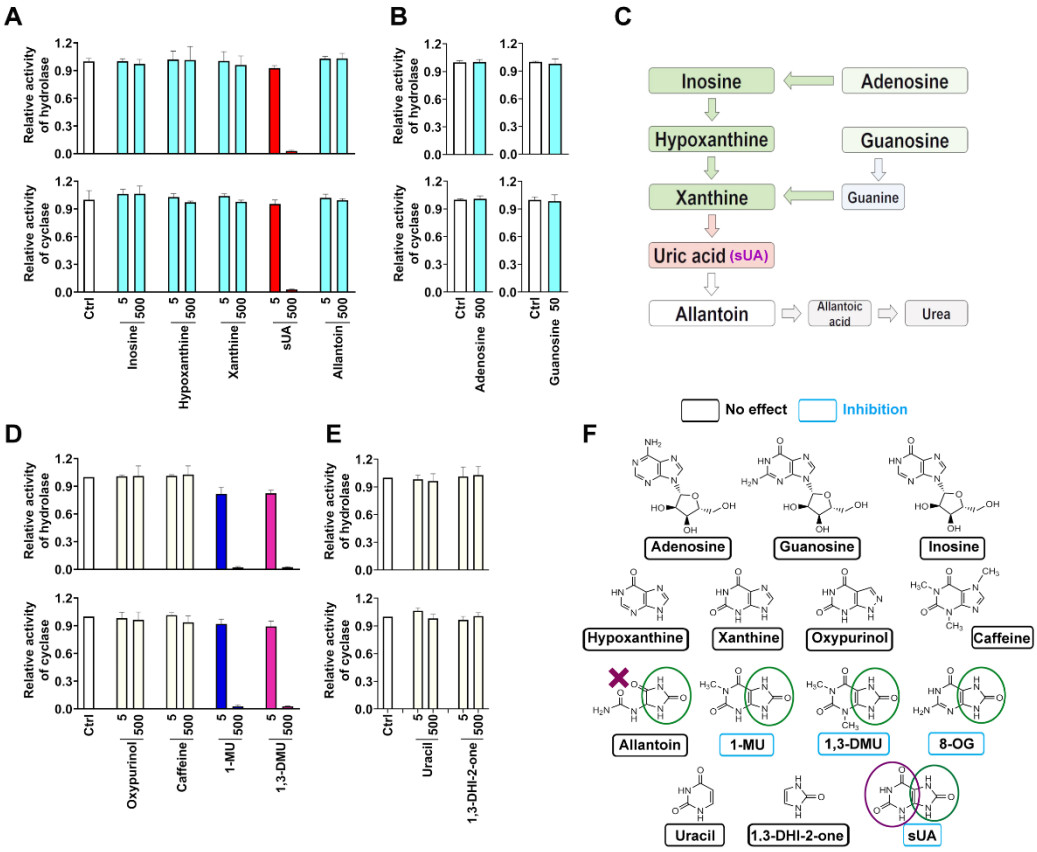

335

336 **Figure 2. CD38 inhibition is restricted to sUA in purine metabolic pathways**
337 (A and B) Effect of sUA precursors and metabolite on hydrolase and cyclase activities
338 of recombinant hCD38. (n = 3 experiments)
339 (C) Major pathways of purine metabolism.
340 (D) Effect of analogs on hydrolase (THP-1 cells) and cyclase (recombinant hCD38)
341 activities. (n = 3 experiments)

342 (E) Effect of uracil and 1,3-dihydroimidazol-2-one (1,3-DHI-2-one) on hydrolase and
343 cyclase activities of recombinant hCD38. (n = 3 experiments)
344 (F) Structural comparison reveals the functional group for CD38 inhibition.
345 Data are mean ± s.d.
346
347

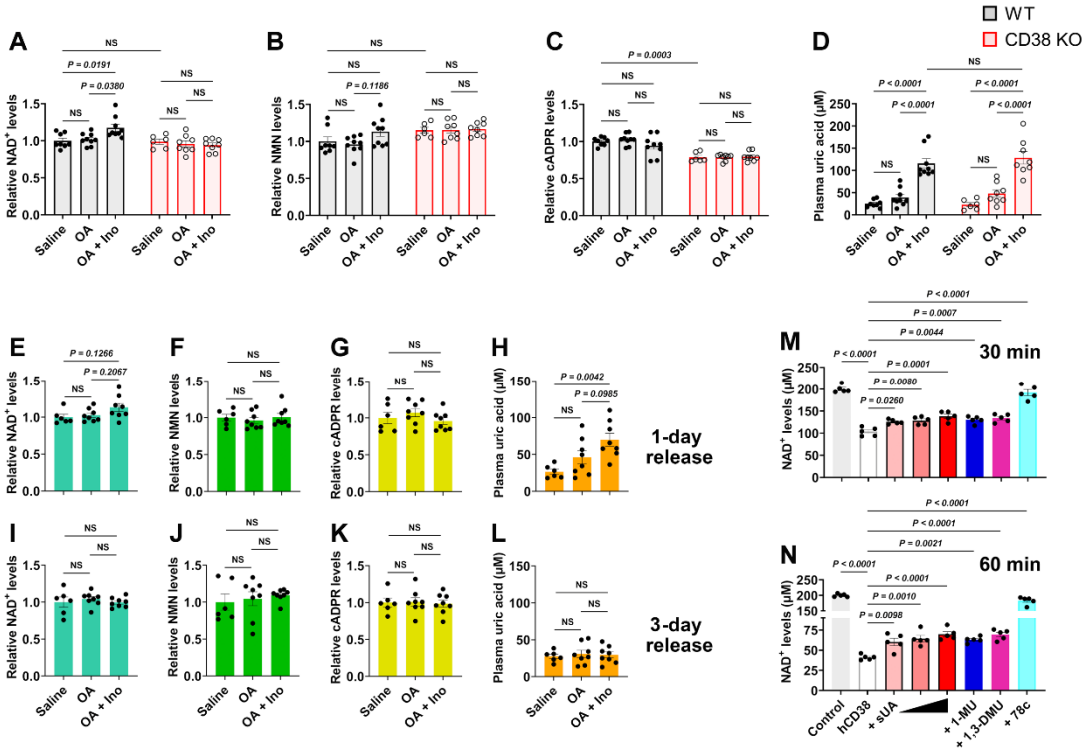

348
349 **Figure 3. sUA limits NAD$^+$ degradation via CD38 inhibition.**
350 WT and CD38 KO mice (10- to 12-week-old) received oral administration of saline,
351 oxonic acid potassium salt (OA), or OA plus inosine (Ino) twice (1-day treatment for
352 sUA elevation). The mice were sacrificed 4 h (A-D), 1 day (E-H), or 3 days (I-L) after
353 the second treatment. Male and female mice were used for these experiments.
354 (A-D) Effect of 1-day treatment (for sUA elevation) on whole blood NAD$^+$ (A), NMN
355 (B), cADPR (C), and plasma sUA (D) levels in WT and CD38 KO mice. (n = 6-9 mice
356 per group)
357 (E-L) Effect of 1-day or 3-day release (after 1-day treatment) on whole blood NAD$^+$,
358 NMN, cADPR, and plasma sUA levels in WT mice of 1-day model. (n = 6-8 mice per
359 group)

(M-N) Effect of sUA (100, 200, or 500 μM) and other ligands (analogs at 500 μM, 78c at 0.5 μM) on NAD^+ degradation by recombinant hCD38. (n = 5 independent samples) Data are mean ± s.e.m. Significance was tested using 2-way ANOVA (A-D), or 1-way ANOVA (E-N) with Tukey's multiple comparisons test. NS, not significant.

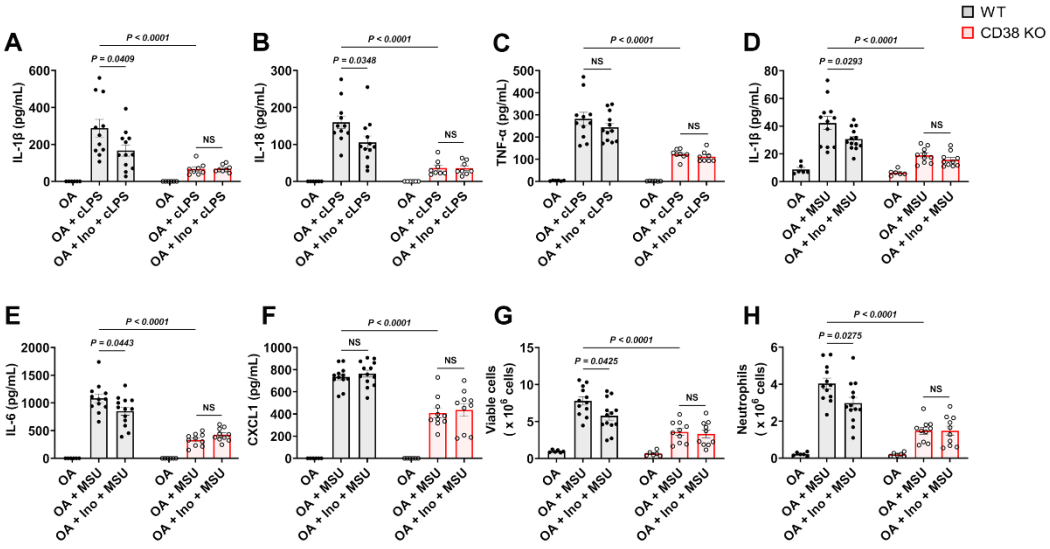

Figure 4. sUA suppresses cLPS-induced systemic inflammation and MSU crystal-induced peritonitis via interacting with CD38

WT and CD38 KO mice (10- to 12-week-old) received oral administration of oxonic acid potassium salt (OA), or OA plus inosine (Ino) twice (1-day sUA elevation). Two hours after the second treatment, mice were intraperitoneally injected with sterile PBS, cLPS (2 mg/kg) or MSU crystals (2 mg/mouse). The mice were sacrificed 6 h after stimulation. Male and female mice were used for these experiments.

(A-C) Effect of 1-day sUA elevation on serum levels of IL-1β (A), IL-18 (B), and TNF-α (C) in cLPS-induced systemic inflammation in WT and CD38 KO mice. (n = 6-12 mice per group)

(D-H) Effect of 1-day sUA elevation on IL-1β (D), IL-6 (E), and CXCL1 (F) levels and recruitment of viable cells (red blood cells excluded) (G) and neutrophils (H) in MSU crystal-induced peritonitis in WT and CD38 KO mice. (n = 6-13 mice per group)

Data are mean ± s.e.m. Significance was tested using 2-way ANOVA with Tukey's

multiple comparisons test. NS, not significant.

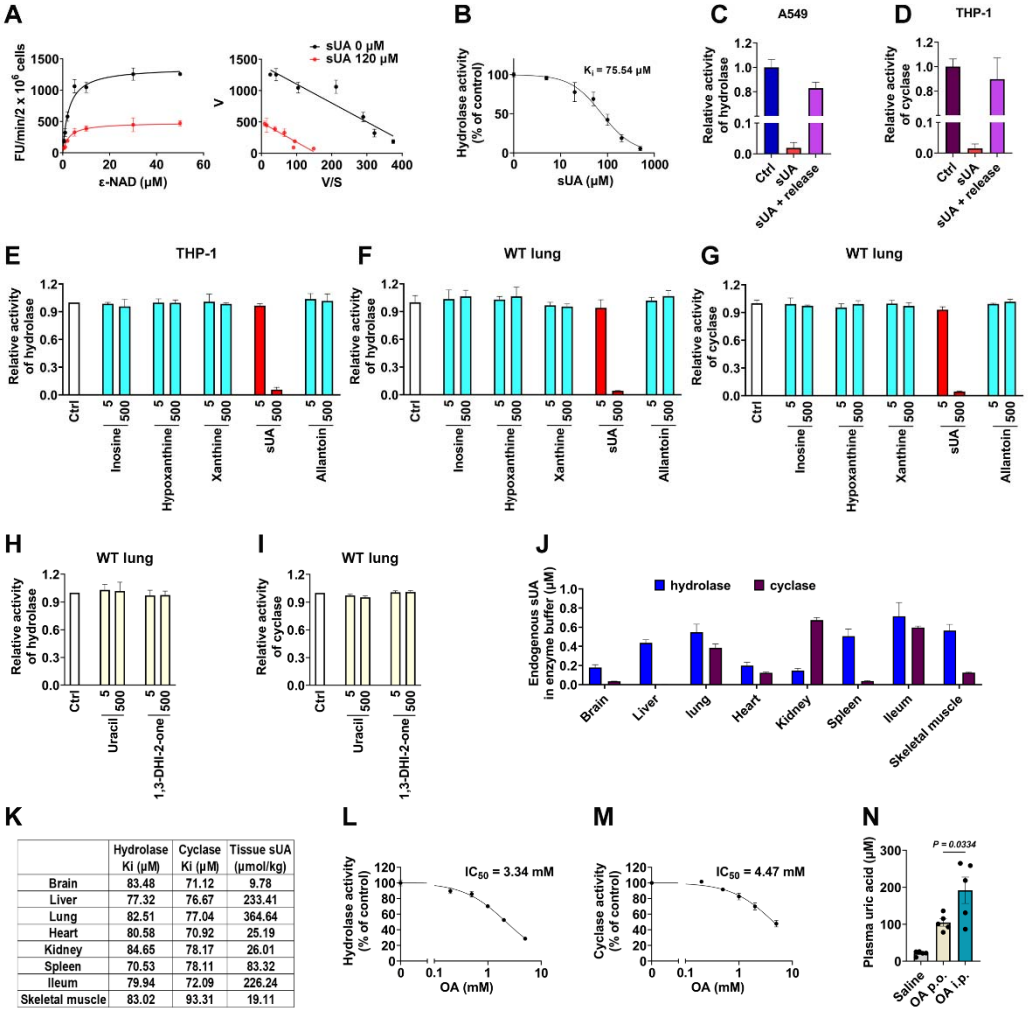

	Hydrolase Ki (μM)	Cyclase Ki (μM)	Tissue sUA (μmol/kg)
Brain	83.48	71.12	9.78
Liver	77.32	76.67	233.41
Lung	82.51	77.04	364.64
Heart	80.58	70.92	25.19
Kidney	84.65	78.17	26.01
Spleen	70.53	78.11	83.32
Ileum	79.94	72.09	226.24
Skeletal muscle	83.02	93.31	19.11

Supplemental Figure S1. Effect of sUA or other ligands on CD38 activity. Related to Fig.1, Fig.2 and Fig.3.

(A) Effect of different ε-NAD$^+$ concentrations on sUA inhibition of hydrolase activity of THP-1 cells. (n = 3 experiments)

(B) Hydrolase activity of THP-1 cells in the presence of sUA (0 to 500 μM). (n = 3 experiments)

(C and D) Reversibility of inhibition of hydrolase (THP-1 cells) (C) and cyclase (A549 cells) (D) by sUA. Naïve THP-1 and A549 cells were incubated with RPMI-1640 medium in the presence or absence of 500 μM sUA for 2 h. Cells were collected and

394 homogenized in reaction buffer on ice with or without 500 μM sUA, samples were then
395 diluted 100-fold in reaction buffer with or without 500 μM sUA for enzyme assay.
396 Control group was not treated with sUA in all steps; sUA group was treated with sUA
397 in each step; sUA release group was treated with sUA prior to dilution in sUA-free
398 buffer for enzyme assays (n = 3 experiments).
399 (E-G) Effect of sUA precursors and metabolite on hydrolase (THP-1 (E) and WT lung
400 tissues (F)) and cyclase (WT lung tissues (G)) activities. (n = 3 experiments)
401 (H and I) Effect of uracil and 1,3-dihydroimidazol-2-one (1,3-DHI-2-one) on hydrolase
402 and cyclase activities of WT lung tissues. (n = 3 experiments)
403 (J) Endogenous sUA concentrations in the final reaction buffer for enzyme assays. sUA
404 levels in initial homogenate or membrane fractions were measured, then the
405 endogenous sUA concentrations in the final reaction buffer were calculated based on
406 loading dilution. (n = 3 biologically independent samples)
407 (K) Comparison between K_i values and mean levels of tissues sUA. K_i values were also
408 shown in Fig.1F, and tissue sUA levels were from WT mice with 1-day treatment of
409 saline (also shown in Fig.S2A).
410 (L and M) Hydrolase and cyclase activities of lung tissues from WT mice in the
411 presence of oxonic acid potassium salt (OA, 0 to 5 mM). (n = 3 experiments)
412 (N) Effect of oxonic acid potassium salt (OA) administration on plasma sUA levels in
413 WT mice that received oral administration of inosine. In saline group, mice received
414 oral administration and intraperitoneal injection of saline. In OA p.o. group, mice
415 received oral administration of inosine (1.5 g/kg) and OA (1.5 g/kg) (the same method
416 used in our models), and intraperitoneal injection of saline. In OA i.p. group, mice
417 received oral administration of inosine (1.5 g/kg), and intraperitoneal injection of OA
418 (0.25 g/kg). Four hours after treatment, plasma sUA was measured. (n = 5 mice per
419 group)
420 Data are mean ± s.d. Significance was tested using 1-way ANOVA with Tukey's
421 multiple comparisons test (N).
422

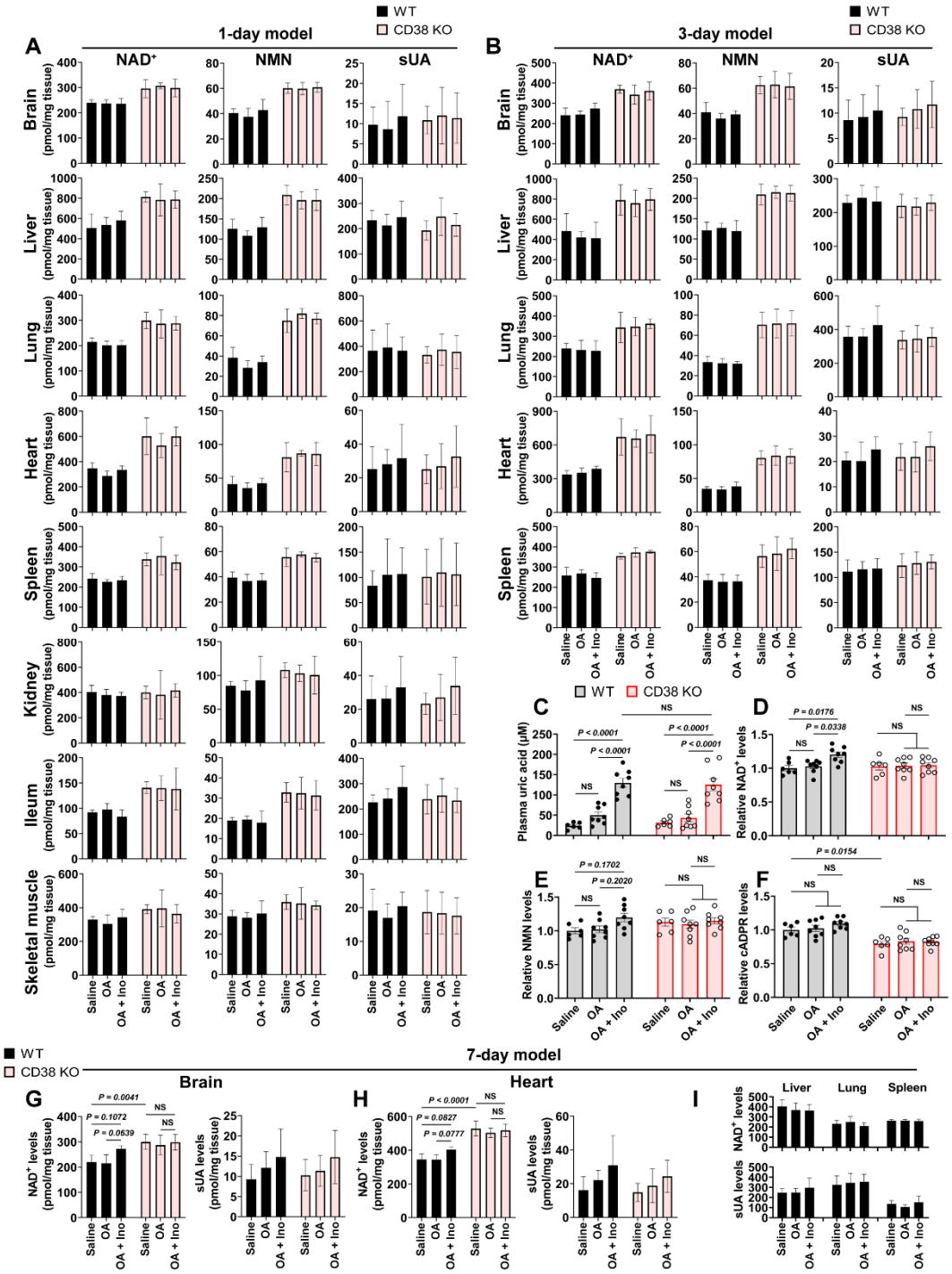

Supplemental Figure S2. Effect of sUA-elevation treatment on tissue NAD$^+$, NMN, and sUA levels. Related to Fig.3

WT and CD38 KO mice (10- to 12-week-old) received oral administration of saline, oxonic acid potassium salt (OA), or OA plus inosine (Ino) twice daily for 1, 3, or 7 days. Four hours after the last treatment, the mice were sacrificed. In 1-day model, the mice

were treated from the evening of day 0 to the morning of day 1.

(A) Effect of 1-day treatment (for sUA elevation) on tissue NAD^+, NMN, and sUA levels. (n = 5 male mice per group)

(B) Effect of 3-day treatment (for sUA elevation) on tissue NAD^+, NMN, and sUA levels. (n = 5 male mice per group)

(C-F) Effect of 3-day treatment (for sUA elevation) on plasma sUA (C), whole blood NAD^+ (D), NMN (E), and cADPR (F) levels. (n = 6-8 mice per group, male and female mice were used in this experiment)

(G-I) Effect of 7-day treatment (for sUA elevation) on tissue NAD^+ and sUA levels. (n = 5 male mice in each group).

Data are mean ± s.d. (A-B and G-I) or mean ± s.e.m. (C-F). Significance was tested using 2-way ANOVA (A-H) with Tukey's multiple comparisons test or 1-way ANOVA (I) with Dunnett's multiple comparisons test.

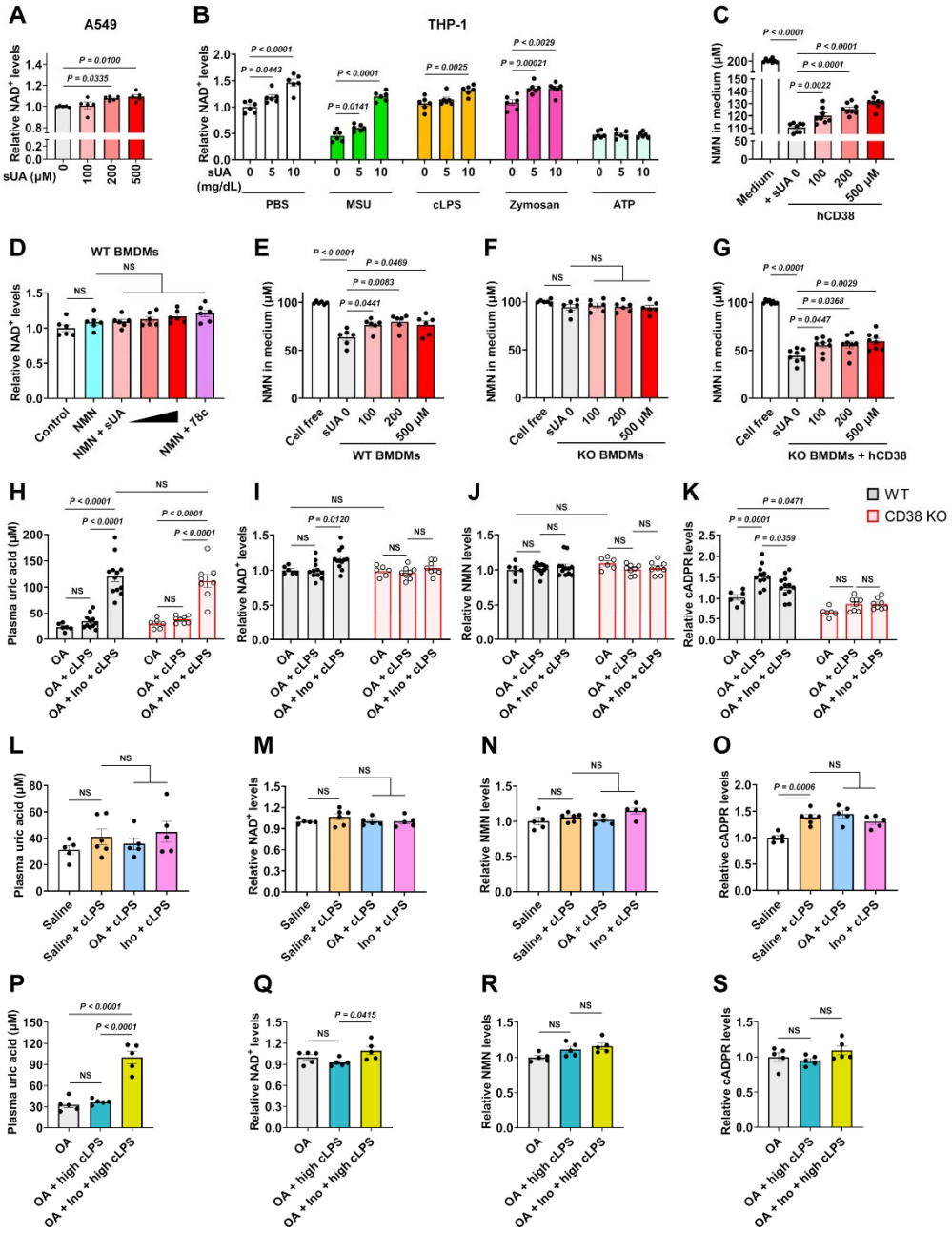

Supplemental Figure S3. Effect of sUA or other treatments on the degradation of NAD^+ and NMN. Related to Fig.3 and Fig.4.

(A) Effect of sUA on intracellular NAD^+ levels of A549 cells. A549 cells were treated with sUA (0-500 μM) in RPMI-1640 medium containing 1% FBS for 20 h. (n = 5 biologically independent samples)

(B) Effect of sUA on intracellular NAD^+ levels of THP-1 cells. Naïve THP-1 cells were incubated with sUA (0-10 mg/dL) in RPMI-1640 medium containing 1% FBS for 2h, then cells were washed twice with PBS and stimulated with MSU crystals (200 μg/mL),

454 cLPS (20 μg/mL), zymosan (50 μg/mL) or ATP (2 mM) for 6 h. (n = 6 biologically
455 independent samples)
456 (C) Effect of sUA on recombinant hCD38-mediated NMN (200 μM) degradation in
457 medium. (n = 8 independent samples)
458 (D) Effect of NMN on intracellular NAD^+ levels of WT BMDMs in the presence or
459 absence of sUA (100, 200, and 500 μM) or 78c (0.5 μM). WT BMDMs were primed
460 with100 ng/mL upLPS for 8 h. (n = 6 biologically independent samples)
461 (E-G) Effect of sUA on extracellular NMN degradation in WT (E) or CD38 KO
462 BMDMs in the absence (F) or presence (G) of recombinant hCD38 (10 ng/mL).
463 BMDMs were primed with 100 ng/mL upLPS for 8 h before metabolic assays. (n = 6
464 biologically independent samples in E and F, n = 8 biologically independent samples in
465 G)
466 (H-K) Effect of 1-day treatment (for sUA elevation) on plasma sUA (H) and whole
467 blood NAD^+ (I), NMN (J), and cADPR (K) levels in WT and CD38 KO mice under
468 inflammatory conditions. Initially, the mice received 1-day treatment (from the evening
469 of day 0 to the morning of day 1) of oxonic acid potassium salt (OA), or OA plus inosine
470 (Ino). Two hours after the last treatment, the mice were intraperitoneally stimulated
471 with sterile PBS or cLPS (2 mg/mL) for 6 h. (n = 6-12 mice per group)
472 (L-O) Effect of 1-day treatment of oxonic acid potassium salt (OA) or inosine (Ino) on
473 plasma sUA (L) and whole blood NAD^+ (M), NMN (N), and cADPR (O) levels in WT
474 mice under inflammatory conditions. The mice received 1-day treatment of OA or Ino
475 (from the evening of day 0 to the morning of day 1). Two hours after the last treatment,
476 the mice were intraperitoneally stimulated with sterile PBS or cLPS (2 mg/mL) for 6 h.
477 (n = 5-6 mice per group)
478 (P-S) Effect of 1-day treatment (for sUA elevation) on plasma sUA (P) and whole blood
479 NAD^+ (Q), NMN (R), and cADPR (S) levels in WT mice stimulated with high-dose
480 cLPS. The mice were treated as mentioned in (H-K) but intraperitoneally stimulated
481 with sterile PBS or cLPS (20 mg/kg) for 4 h. (n = 5 mice per group)
482 Data are mean ± s.e.m. Significance was tested using 1-way ANOVA with Dunnett's

483 (A-B) or Tukey's (C-G, and L-S) multiple comparisons test, or 2-way ANOVA with

484 Tukey's multiple comparisons test (H-K).

485

486

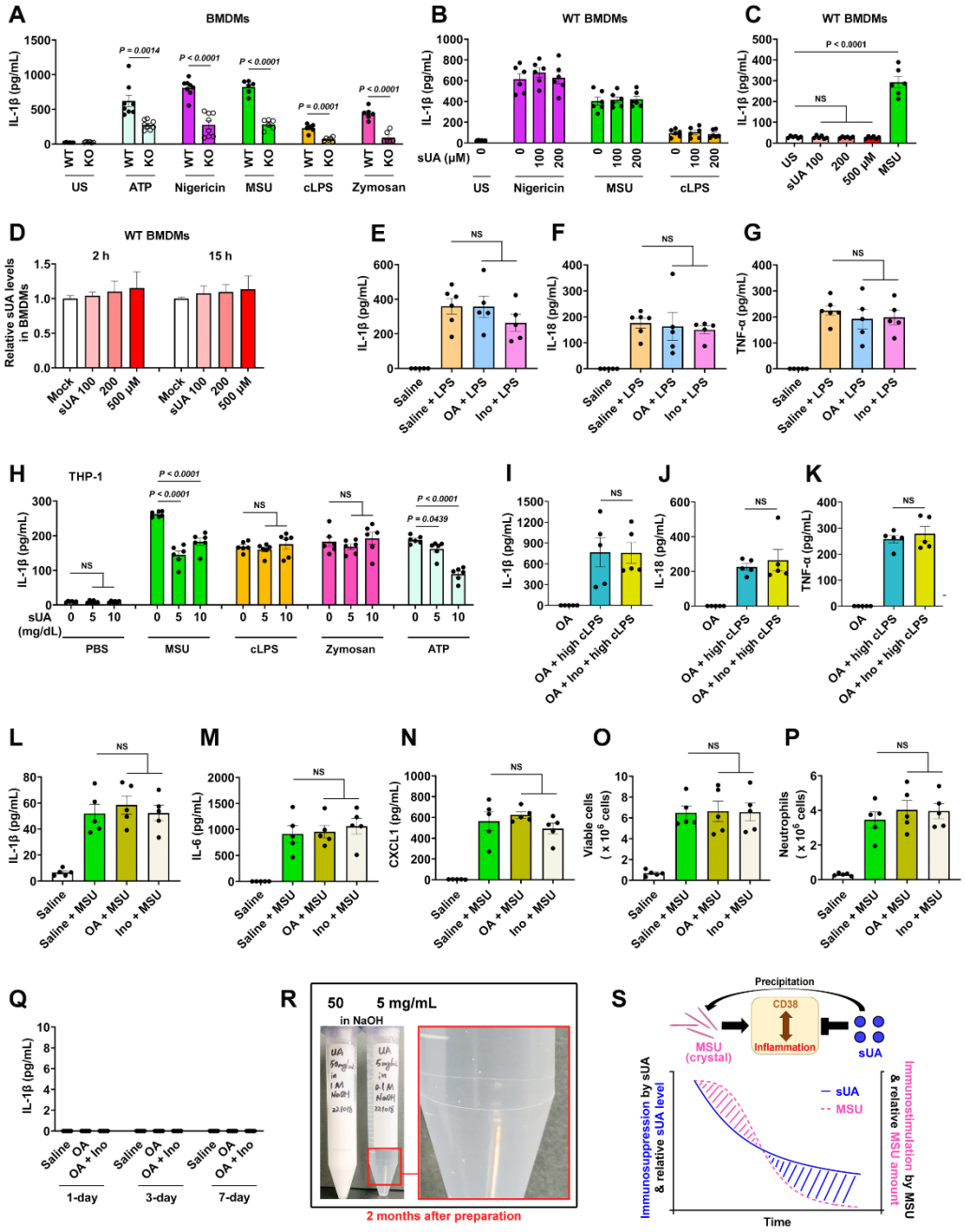

487

488 **Supplemental Figure S4. Effect of sUA or other treatments on innate immunity.**

489 **Related to Fig.4.**

490 (A) Effect of CD38 KO on IL-1β release in primed BMDMs. WT and KO BMDMs

were primed with 100 ng/mL upLPS for 4 h, then primed BMDMs were challenged by ATP (5 mM, 30min), nigericin (3 μM, 2 h), MSU crystals (200 μg/mL, 6 h), cLPS (20 μg/mL, 6 h), and zymosan (50 μg/mL, 4 h). US means unstimulated. (n = 8 biologically independent samples in ATP and nigericin groups, n = 6 biologically independent samples in the remaining groups)

(B-D) Effect of sUA pre-incubation on IL-1β release and intracellular sUA levels in primed BMDMs. WT BMDMs were primed with 100 ng/mL upLPS for 4 h. In (B), the cells were pre-incubated with or without sUA (100 or 200 μM) for 2 h. Then, cells were washed twice with PBS and stimulated with nigericin (3 μM, 2 h), MSU crystals (200 μg/mL, 4 h), or cLPS (1 μg/mL, 4 h). In (C and D), primed BMDMs were directly stimulated with sUA (100, 200, and 500 μM) or MSU crystals (100 μg/mL) for 6 h. US means unstimulated. (n = 6 biologically independent samples in B and C, n = 3 biologically independent samples in D)

(E-G) Effect of 1-day treatment of oxonic acid potassium salt (OA) or inosine (Ino) on cLPS-induced systemic inflammation in WT mice. Initially, the mice received 1-day treatment (from the evening of day 0 to the morning of day 1). Two hours after the second treatment, the mice were intraperitoneally stimulated with sterile PBS or cLPS (2 mg/mL) for 6 h, serum IL-1β (E), IL-18 (F), and TNF-α (G) levels were measured. (n = 5-6 mice per group)

(H) THP-1 cells were primed with 0.5 μM PMA for 3 h the day before stimulation. Primed THP-1 cells were pre-incubated with sUA (0-10 mg/dL) for 2 h, then cells were washed twice with PBS and challenged by MSU crystals (200 μg/mL), cLPS (20 μg/mL), zymosan (50 μg/mL), and ATP (2 mM) for 4 h. (n = 6 biologically independent samples)

(I-K) Effect of 1-day treatment (for sUA elevation) on high-dose cLPS-induced systemic inflammation in WT mice. The mice received 1-day treatment (from the evening of day 0 to the morning of day 1) of oxonic acid potassium salt (OA), or OA plus inosine (Ino). Two hours after the last treatment, the mice were intraperitoneally stimulated with sterile PBS or cLPS (20 mg/mL) for 4 h, serum IL-1β (I), IL-18 (J), and

TNF-α (K) levels were measured. (n = 5 mice per group)

(L-P) Effect of 1-day treatment of oxonic acid potassium salt (OA) or inosine (Ino) on MSU crystal-induced peritonitis in WT mice. The mice were treated as described in (E-G) but intraperitoneally stimulated with sterile PBS or MSU crystals (2 mg/mouse) for 6 h. IL-1β (L), IL-6 (M), CXCL-1 (N), and the number of viable cells (red blood cells excluded) (O) and neutrophils (P) in peritoneal lavage fluid were detected. (n = 5 mice per group)

(Q) Effect of 1- to 7-day treatment (for sUA elevation) on serum IL-1β levels. (n = 5 mice per group)

(R) Crystals precipitation in sUA stock solution. 50 mg/mL of sUA in 1 M NaOH and 5 mg/mL of sUA in 0.1 M NaOH were prepared without pH adjustment. Crystals were immediately precipitated after dissolution in 50 mg/mL tube. Visible crystals were observed in 5 mg/mL tube two months after storage at 4 ℃.

(S) Hypothesis for the remodeling of innate immunity by the balance between sUA and MSU crystals in gout patients.

Data are mean ± s.e.m. (A-C, and E-Q) or mean ± s.d. (D). Significance was tested using two-tailed unpaired t-test (A), 1-way ANOVA with Dunnett's (B-D, H and Q) or Tukey's (E-G, and I-P) multiple comparisons test.

RESOURCE AVAILABILITY

Lead contact

Further information and requests for resources and reagents should be directed to the lead contact Ikumi Tamai (tamai@p.kanazawa-u.ac.jp).

Materials availability

This study did not generate new unique reagents.

Data and code availability

All data reported in this paper will be shared by the lead contact upon request.

This paper does not report original code.

Any additional information required to reanalyze the data reported in this paper is available from the lead contact upon request.

EXPERIMENTAL MODEL AND STUDY PARTICIPANT DETAILS

Animal models

Male and female ICR (Institute of Cancer Research of the Charles River Laboratories, Inc., Wilmington, MA, USA) mice were initially purchased from Japan SLC, Inc. (Hamamatsu, Japan). CD38 KO mice (ICR strain) were generated using the CRISPR/Cas9 method as previously described[59]. WT and CD38 KO mice were kept and bred at the Experimental Animal Center of Kanazawa University (Takara-machi campus). For animal experiments, all the mice (sex and age as indicated in respective figure legends) were transferred a week in advance and housed in the animal room of Research Center of Child Mental Development under standard conditions (24 °C; 12 h light/dark cycle, lights on at 8:30 am) with standard chow and water provided *ad libitum*. Male and female mice were separated after weaning and equally used for experiments except when specified. In each experimental group, the mice were from different biological mothers. All animal experiments were approved by the Institutional Animal Care and Use Committee at Kanazawa University (AP-214243), and were performed in accordance with the local guidelines.

Cell culture

THP-1 and A549 cells were cultured in RPMI-1640 containing 10% FBS and 1% penicillin/streptomycin. Bone marrow cells and bone marrow-derived macrophages were maintained in RPMI-1640 containing 10% FBS, 1% penicillin/streptomycin, and 50 μM 2-mercaptoethanol in the presence or absence of macrophage colony stimulating factor (M-CSF).

METHOD DETAILS

578 **Mild elevation of sUA in mice**

579 For 1-day elevation of plasma sUA, WT and CD38 KO mice received oral
580 administration of saline, oxonic acid potassium salt (1.5 g/kg), or inosine (1.5 g/kg)
581 plus oxonic acid potassium salt (1.5 g/kg), the gavage volume was 5 mL/kg. Drug
582 suspension in saline was freshly prepared and warmed to 37 ℃ before each treatment.
583 The mice received the first treatment on the evening (19:00) of the first day, and the
584 second treatment on the morning (9:00) of the second day (experimental day). For 3-
585 day or 7-day elevation of plasma sUA, WT and CD38 KO mice received the same
586 treatment twice daily from the evening of the first day to the morning of the last day.
587 Four hours after the last treatment, the mice were sacrificed, and whole blood, serum,
588 plasma, and tissues were collected for metabolic studies. For immunological studies,
589 mice were stimulated 2 h after the second treatment on the morning (9:00) of the second
590 day.

591

592 **sUA release in mice**

593 WT mice received oral administration of saline, oxonic acid potassium salt, or
594 inosine plus oxonic acid potassium salt (1-day model, as described above). One day or
595 3 days after the second treatment, the mice were sacrificed, and whole blood and plasma
596 were collected for metabolic studies.

597

598 **Crude LPS-induced systemic inflammation**

599 WT and CD38 KO mice received 1-day elevation of plasma sUA as described
600 above. Two hours after the last treatment, the mice were intraperitoneally injected with
601 sterile PBS or cLPS (2 mg/kg or 20 mg/kg), and the injection volume was 3 mL/kg.
602 Four hours (20 mg/kg) or 6 h (2 mg/kg) after stimulation, the mice were sacrificed, and
603 whole blood, plasma, and serum were collected for metabolic and immunological
604 studies.

605

606 **MSU crystal-induced peritonitis**

607 WT and CD38 KO mice received 1-day elevation of plasma sUA as described
608 above. Two hours after the last treatment, the mice were intraperitoneally injected with
609 sterile PBS or MSU crystals (2 mg/mouse), and the injection volume was 200 μL/mouse.
610 Six hours after stimulation, the mice were sacrificed and blood samples were collected.
611 For each mouse, the peritoneal cavity was washed with 5 mL ice-cold sterile PBS, the
612 supernatant was collected by centrifugation for subsequent ELISA, and cell pellets were
613 used for total viable cell count by Trypan Blue staining and neutrophil count by Wright-
614 Giemsa staining. In brief, cell pellet from 1.5 mL of peritoneal lavage fluid was
615 resuspended in red blood cell lysis buffer for 30 s, PBS (9-fold volume) was added to
616 terminate lysis. Afterward, the cells were centrifuged at 1000 rpm for 5 min and
617 resuspended in PBS for viable cell count. For neutrophil count, peritoneal lavage fluid
618 was directly used for smears after appropriate dilution, and subsequently, Wright-
619 Giemsa staining was performed according to the protocols provided by the
620 manufacturer. Viable cells and neutrophils were counted by two investigators, and the
621 mean numbers were shown in the figures and Source Data.
622
623 **Handling of animal samples**
624 The collected whole blood samples were immediately diluted 10-fold in 5% ice-
625 cold perchloric acid (PCA) and homogenized on ice. After 10-min centrifugation at
626 15000 rpm, 4 ℃, the supernatant was subpackaged for measurement or -80 ℃ storage.
627 For NAD^+ measurement in whole blood, the supernatant was handled without freezing
628 and thawing, and measured within 24 h of sample collection. For measurement of
629 plasma sUA, after sample collection, we immediately diluted the plasma with 5% ice-
630 cold PCA, after vortex, samples were centrifuged at 15000 rpm, 4 ℃ for 10 min, the
631 collected supernatant was used for the subsequent handling and measurement within 24
632 h.
633 After the collection of blood samples (whole blood and plasma), the mice were
634 immediately perfused with ice-cold PBS. The tissue samples were collected, dried with
635 tissue paper, and weighed. All the tissue samples were immediately homogenized in 5%

ice-cold PCA on ice, then centrifuged at 15000 rpm, 4℃ for 10 min. The supernatant was collected and stored at -80 ℃ until further handling for measurement (see LC-MS/MS analysis).

Preparation of MSU crystal and sUA solution

MSU crystals were prepared by the recrystallization of oversaturated sUA according to a previous report[8]. Improper preparation of sUA solution may introduce crystals to cause false-positive or false-negative results. It has been demonstrated that crystals may precipitate in sUA solution prepared by pre-warming to stimulate immune cells to secrete cytokines[12]. In this study, the sUA solution was prepared according to an improved protocol[12]. Briefly, we directly dissolved sUA at 0.5 mg/mL in blank RPMI-1640 medium by addition of NaOH, and adjusted the pH by HCl. Then sUA solution was immediately filtered by 0.2-μm filters and diluted to experimental concentration (up to 10 mg/L, 595 μM). For all experiments, sUA solution was freshly prepared and used immediately.

Preparation of BMDMs

Bone marrow-derived macrophages (BMDMs) were prepared and primed as previously described[56]. In brief, bone marrow cells were isolated from 10- to 12-week-old WT or CD38 KO mice by washing the marrow cavity with sterile PBS. The collected bone marrow cells were filtered by 70-μm strainers and then centrifuged at 1000 rpm, 4℃ for 5 min. The cell pellet was resuspended in 2 mL RBC lysis buffer for 30 s, then 8 mL complete RPMI-1640 medium (10% FBS, 1% Penicillin/Streptomycin and 50 μM 2-mercaptoethanol) was added to terminate the lysis. After 5-min centrifugation at 1000 rpm, 4℃, the cells were resuspended in fresh complete RPMI-1640 medium and maintained for 4 h in an incubator. Adherent cells were discarded, whereas non-adherent cells were cultured in complete RPMI-1640 medium containing 20 ng/mL M-CSF. After 3-day differentiation, the medium was replaced with fresh complete RPMI-1640 medium containing 20 ng/mL M-CSF. On the 7th day, BMDMs

665 were collected for subsequent experiments. BMDMs were primed with 100 ng/mL
666 ultrapure LPS (upLPS) for 4 h for canonical inflammasome assay. For metabolic assay
667 of NMN, BMDMs were primed with 100 ng/mL upLPS for 8 h to induce higher protein
668 expression of CD38.
669
670 **Intracellular NAD^+ assay**
671 A549 cells were seeded in 24-well plates for NAD^+ assay. Briefly, when the
672 confluence reached 80%, the culture medium in each well was discarded, and the cells
673 were washed twice with PBS and incubated in RPMI-1640 medium containing 1% FBS
674 in the presence or absence of sUA (from 100 to 500 μM) for 20 h. Then the cells were
675 washed twice with PBS, after the second washing, PBS was completely removed and
676 100 μL 5% ice-cold PCA was added into each well. The plate was kept on ice for 2 h,
677 then cell samples were collected and centrifuged at 15000 rpm, 4°C for 10 min. The
678 supernatant was used for subsequent handling and measurement (see LC-MS/MS
679 analysis).
680 Non-primed THP-1 cells were pre-incubated in RPMI-1640 medium in the
681 presence or absence of sUA (5 or 10 mg/dL) for 2 h. The cells were washed twice with
682 PBS, and incubated with the inflammatory stimuli for 6 h. Subsequently, the cells were
683 washed twice with PBS, and then a total of 100 μL 5% ice-cold PCA was used to extract
684 NAD^+ from cells in each well and medium as mentioned above.
685 WT BMDMs were primed with 100 ng/mL upLPS for 8 h. Then the cells were
686 washed twice with PBS. Afterward, the cells were incubated in control or 100 μM
687 NMN-supplemented RPMI-1640 medium in the presence of sUA or 78c. After 6-h
688 incubation, the cells were washed twice with PBS. Finally, cell samples for NAD^+
689 measurement were collected by 5% ice-cold PCA as mentioned above.
690
691 **Canonical inflammasome assay**
692 Naïve THP-1 cells were primed with phorbol 12-myristate 13-acetate (PMA) at 0.5
693 μM for 3 h the day before stimulation. Primed THP-1 cells were pre-incubated in

694 RPMI-1640 medium in the presence or absence of sUA (5 or 10 mg/dL) for 2 h. The
695 cells were then washed twice with PBS, and stimulated with different ligands in serum-
696 free RPMI-1640 medium for 4 h.

697 WT and CD38 KO BMDMs were primed with 100 ng/mL upLPS for 4 h.
698 Subsequently, primed BMDMs were pre-incubated with or without sUA (5 or 10 mg/dL)
699 for 2 h, the cells were then washed twice with PBS and stimulated with ligands in
700 serum-free RPMI-1640 medium.

701 After stimulation, the culture medium was collected and centrifuged at 3000 rpm,
702 4 ℃ for 5 min, and the supernatant was collected and stored at -30 ℃ until ELISA.

703

704 **sUA uptake assay**

705 WT BMDMs were primed with 100 ng/mL upLPS for 4 h. Then the cells were
706 washed twice with PBS, and maintained in RPMI-1640 medium containing sUA (100,
707 200, or 500 μM) for 2 h or 15 h. Subsequently, the cells were washed twice with ice-
708 cold PBS to terminate uptake, 100 μL 5% ice-cold PCA was added into each well. The
709 plates were placed on ice for 2 h, then cell samples were collected and centrifuged at
710 15000 rpm, 4℃ for 10 min. The supernatant was used for subsequent handling and
711 measurement (see LC-MS/MS analysis).

712

713 **ELISA**

714 Human IL-1β, mouse IL-1β, IL-6, IL-18, TNFα and CXCL1 levels were measured
715 according to the protocols provided by the manufacturer. Samples were diluted using
716 the buffer provided in the kits before the assays when applicable. In this study, all the
717 samples were frozen after collection and thawed before ELISA.

718

719 **Measurement of CD38 activity**

720 CD38 hydrolase activity was measured using 50 μM ε-NAD as a substrate in
721 hydrolase reaction buffer (250 mM sucrose, 40 mM Tris-HCl, pH 7.4) according to a
722 previous report[60]. Briefly, cells or tissues were directly homogenized in blank reaction

723 buffer on ice, and recombinant hCD38 was diluted in blank reaction buffer for
724 subsequent assays. The tissue homogenates were centrifuged to collect the supernatant
725 for enzyme assays. The loading volume of enzyme was 4 to 30 μL, while the total
726 volume of the reaction system was 3 mL. To detect enzyme inhibition, except when
727 specified, the ligands were directly dissolved in hydrolase reaction buffer before pH
728 adjustment, after which, the pH was immediately adjusted to 7.4. All reaction buffers,
729 with or without ligands, were freshly prepared before each assay. For measurement of
730 hydrolase activity, 3 mL reaction buffer containing enzyme, ε-NAD, and ligands at
731 indicated concentrations was maintained at 37 °C with constant stirring.

732 CD38 cyclase activity was measured using 60 μM NGD as a substrate in cyclase
733 reaction buffer (100 mM KCl, 10 μM $CaCl_2$ and 50 mM Tris-HCl, pH 6.6) as previously
734 described[19,61]. Tissues were cut into pieces and suspended in lysis buffer (5 mM $MgCl_2$,
735 10 mM Tris-HCl, pH 7.3) at 4 °C for 30 min. Then, the suspension was homogenized
736 on ice, and the supernatant was collected after centrifugation. To collect the crude
737 membrane fractions, the supernatant was centrifuged at 105000 g for 30 min. The final
738 pellet was resuspended in 10 mM Tris-HCl solution (pH 6.6) for cyclase assay.
739 Homogenates of THP-1 or A549 cells, and recombinant hCD38 were used directly for
740 cyclase assays. The loading volume of enzyme was 4 to 20 μL, while the total volume
741 of reaction system was 3 mL. To detect enzyme inhibition, except when specified, the
742 ligands were directly dissolved in cyclase reaction buffer before pH adjustment, after
743 which, the pH was immediately adjusted to 6.6. All reaction buffers, with or without
744 ligands, were freshly prepared before each assay. For measurement of cyclase activity,
745 3 mL reaction buffer containing enzyme, NGD and ligands at indicated concentrations
746 was maintained at 37 °C with constant stirring.

747 The reaction buffer for hydrolase or cyclase assays was excited at 300 nm, and
748 fluorescence emission was measured every second at 410 nm by Shimazu RF-6000
749 spectrofluorometer. Hydrolase or cyclase activity was calculated from the linear portion
750 of the time course by fitting a linear function to the data points recorded within 5 min.

751 In this study, 8-OG and guanosine were tested only at 50 μM due to the limited

752 solubility. Guanosine was dissolved in DMSO and diluted in the reaction buffer for
753 subsequent assays.
754 For reversibility test, recombinant hCD38 was pre-incubated for 30 min in 4
755 conditions: (1) control reaction buffer; (2) in the presence of 100 μM substrate (ε-NAD^+
756 or NGD); (3) 500 μM sUA; (4) both substrate and sUA. Subsequently, the enzyme was
757 diluted 100-fold in reaction buffer in the presence or absence of 500 μM sUA for
758 activity assays using ε-NAD^+ or NGD.
759
760 **Metabolic assay of NAD^+**
761 NAD^+ degradation by recombinant hCD38 was detected in hydrolase reaction
762 buffer. At first, sUA (100, 200 and 500 μM) or indicated ligands at 500 μM in hydrolase
763 reaction buffer (250 mM sucrose, 40 mM Tris) was newly prepared, then the pH was
764 immediately adjusted to 7.4 by HCl. Recombinant hCD38 was added into the buffer of
765 experimental groups at 20 ng/mL, then the buffer was maintained at 37 ℃. The
766 substrate NAD^+ was dissolved in hydrolase reaction buffer (pH 7.4) at 10 mM, and the
767 pH was further adjusted to 7.4. The reaction was started with the addition of NAD^+ in
768 the buffer for each group (final concentration is 200 μM), including control group
769 (recombinant hCD38 free). All the buffer was incubated at 37 ℃ with constant stirring.
770 After 30 or 60 min, 20 μL reaction buffer was transferred into 180 μL of 5% ice-cold
771 PCA, then vortexed for 30 s before 10-min centrifugation at 15000 rpm, 4 ℃. The
772 supernatant was further handled for NAD^+ measurement within 12 h without freezing
773 and thawing (see LC-MS/MS analysis).
774
775 **Metabolic assay of NMN**
776 To prepare the reaction buffer, sUA was directly dissolved in blank RPMI-1640
777 medium by addition of NaOH, and the pH was immediately adjusted by HCl. After pH
778 adjustment, the medium containing sUA was filtered by 0.2-μm filter and diluted as
779 indicated. The medium containing 20 ng/mL recombinant hCD38 was then placed in a
780 cell incubator. The reaction was started with the addition of NMN (final concentration

781 was 200 μM). After incubation for 6 h, 20 μL medium was transferred into 180 μL 5%
782 ice-cold PCA, then vortexed for 30 s and centrifuged at 15000 rpm, 4 °C for 10 min.
783 The supernatant was stored at -80 °C until further handling for NMN measurement (see
784 LC-MS/MS analysis).
785
786 **Extracellular NMN degradation**
787 sUA (0, 100, 200, and 500 μM) was prepared in blank RPMI-1640 medium. WT
788 and CD38 KO BMDMs were primed with 100 ng/mL upLPS for 8 h, then the cells
789 were washed twice with PBS. Primed BMDMs were maintained in RPMI-1640
790 medium supplemented with 100 μM NMN in the presence or absence of sUA. To
791 restore the inhibitory effects of sUA on NMN degradation in KO BMDMs, recombinant
792 hCD38 was added to the medium (final concentration was 10 ng/mL). After 6-h
793 incubation, culture medium was collected and centrifuged at 3000 rpm, 4 °C for 5 min.
794 20 μL of supernatant was transferred into 180 μL 5% ice-cold PCA, then vortexed for
795 30 s and centrifuged at 15000 rpm, 4 °C for 10 min. The supernatant was stored at -80 °C
796 until further handling for NMN measurement.
797
798 **LC-MS/MS analysis**
799 As mentioned above, samples (cells, tissues, blood or reaction buffer) were treated
800 with ice-cold PCA, after extraction and centrifugation, the collected supernatant was
801 appropriately diluted in 5% ice-cold PCA, and then vortexed for 30 s and centrifuged
802 at 15000 rpm, 4°C for 5 min. 30 μL supernatant was added into 200 μL 5 mM
803 ammonium formate containing internal standards at indicated concentrations. Then all
804 the samples were vortexed for 30 s and centrifuged at 15000 rpm, 4°C for 5 min again,
805 the final supernatant was used for subsequent measurement. All the handled samples
806 were immediately analyzed in this study without freezing and thawing.
807 The LC-MS/MS system consisted of a triple quadrupole LCMS-8050 (Shimadzu,
808 Kyoto, Japan) and an LC-30A system (Shimadzu, Kyoto, Japan). NAD^+, NMN and the
809 N-cyclohexyl benzamide (NCB, internal standard, 5 ng/mL) were eluted on Altlantis®

HILIC Silica (2.1 × 150 mm, 5 μm) at 40 °C using an isocratic mobile phase containing 60% water with 0.1% formic acid and 40% acetonitrile with 0.1% formic acid at 0.4 mL/min. The selected transitions of m/z were 664.10 → 136.10 for NAD^+, 334.95 → 123.15 for NMN, and 204.10 → 122.20 for NCB in positive ion mode. NAD^+ and NMN were measured independently in this study, as their peaks were hardly separated within a short time.

sUA, cADPR and FYU-981 (internal standard, 1 μM) were eluted on CAPCELL PAK C8 TYPE UG 120 (2 × 150 mm, 5 μm) at 40 °C. sUA and FYU-981 were separated using a gradient mobile phase containing water with 0.1% formic acid (A) and acetonitrile with 0.1% formic acid (B) at 0.4 mL/min. The elution was started with 55% A for 0.5 min, A was decreased from 55% to 5% for 1 min, then A was increased from 5% to 55% for 0.5 min, finally 55% A was maintained for 0.5 min. cADPR and FYU-981 were separated using an isocratic mobile phase containing 60% water with 0.1% formic acid and 40% acetonitrile with 0.1% formic acid at 0.4 mL/min. The selected transitions of m/z were 167.10 → 124.10 for sUA, 539.95 → 272.95 for cADPR, and 355.95 → 159.90 for FYU-981 in negative ion mode.

The injection volume was 1 μL for all measurements, and data manipulation was accomplished by Labsolutions software (version 5.97, Shimadzu, Kyoto, Japan).

QUANTIFICATION AND STATISTICAL ANALYSIS

Statistics were performed using GraphPad Prism 9.5.1. Sample size was not predetermined by any statistical methods. Single comparisons between two groups were made by two-tailed unpaired t-test. Comparisons between multiple groups were performed using 1-way ANOVA with Dunnett's or Tukey's multiple comparisons test or 2-way ANOVA with Tukey's multiple comparisons test when applicable. Data were shown as mean ± s.e.m. or mean ± s.d. as indicated. Statistical tests and parameters were reported in figure legends. $p < 0.05$ was considered significant.

Reference

1. Wu, X.W., Muzny, D.M., Lee, C.C., and Caskey, C.T. (1992). Two independent mutational events in the loss of urate oxidase during hominoid evolution. J Mol Evol. *34*, 78-84. 10.1007/bf00163854.
2. Oda, M., Satta, Y., Takenaka, O., and Takahata, N. (2002). Loss of urate oxidase activity in hominoids and its evolutionary implications. Mol Biol Evol. *19*, 640-653. 10.1093/oxfordjournals.molbev.a004123.
3. Hosomi, A., Nakanishi, T., Fujita, T., and Tamai, I. (2012). Extra-renal elimination of uric acid via intestinal efflux transporter BCRP/ABCG2. PloS one *7*, e30456. 10.1371/journal.pone.0030456.
4. Watanabe, S., Kang, D.H., Feng, L., Nakagawa, T., Kanellis, J., Lan, H., Mazzali, M., and Johnson, R.J. (2002). Uric acid, hominoid evolution, and the pathogenesis of salt-sensitivity. Hypertension. *40*, 355-360. 10.1161/01.hyp.0000028589.66335.aa.
5. Glantzounis, G.K., Tsimoyiannis, E.C., Kappas, A.M., and Galaris, D.A. (2005). Uric acid and oxidative stress. Curr Pharm Des. *11*, 4145-4151. 10.2174/138161205774913255.
6. Dehlin, M., Jacobsson, L., and Roddy, E. (2020). Global epidemiology of gout: prevalence, incidence, treatment patterns and risk factors. Nat Rev Rheumatol. *16*, 380-390. 10.1038/s41584-020-0441-1.
7. Howles, S.A., and Thakker, R.V. (2020). Genetics of kidney stone disease. Nat Rev Urol. *17*, 407-421. 10.1038/s41585-020-0332-x.
8. Martinon, F., Pétrilli, V., Mayor, A., Tardivel, A., and Tschopp, J. (2006). Gout-associated uric acid crystals activate the NALP3 inflammasome. Nature *440*, 237-241. 10.1038/nature04516.
9. Shi, Y., Evans, J.E., and Rock, K.L. (2003). Molecular identification of a danger signal that alerts the immune system to dying cells. Nature *425*, 516-521. 10.1038/nature01991.
10. Shi, Y. (2010). Caught red-handed: uric acid is an agent of inflammation. J Clin Invest. *120*, 1809-1811. 10.1172/jci43132.

11. Alberts, B.M., Barber, J.S., Sacre, S.M., Davies, K.A., Ghezzi, P., and Mullen, L.M. (2019). Precipitation of Soluble Uric Acid Is Necessary for In Vitro Activation of the NLRP3 Inflammasome in Primary Human Monocytes. J Rheumatol. *46*, 1141-1150. 10.3899/jrheum.180855.

12. Ma, Q., Honarpisheh, M., Li, C., Sellmayr, M., Lindenmeyer, M., Böhland, C., Romagnani, P., Anders, H.J., and Steiger, S. (2020). Soluble Uric Acid Is an Intrinsic Negative Regulator of Monocyte Activation in Monosodium Urate Crystal-Induced Tissue Inflammation. J Immunol. *205*, 789-800. 10.4049/jimmunol.2000319.

13. Ma, Q., Immler, R., Pruenster, M., Sellmayr, M., Li, C., von Brunn, A., von Brunn, B., Ehmann, R., Wölfel, R., Napoli, M., et al. (2022). Soluble uric acid inhibits β2 integrin-mediated neutrophil recruitment in innate immunity. Blood *139*, 3402-3417. 10.1182/blood.2021011234.

14. Kono, H., Chen, C.J., Ontiveros, F., and Rock, K.L. (2010). Uric acid promotes an acute inflammatory response to sterile cell death in mice. J Clin Invest. *120*, 1939-1949. 10.1172/jci40124.

15. Cantor, J.R., Abu-Remaileh, M., Kanarek, N., Freinkman, E., Gao, X., Louissaint, A., Jr., Lewis, C.A., and Sabatini, D.M. (2017). Physiologic Medium Rewires Cellular Metabolism and Reveals Uric Acid as an Endogenous Inhibitor of UMP Synthase. Cell *169*, 258-272.e217. 10.1016/j.cell.2017.03.023.

16. Chini, E.N., Chini, C.C.S., Espindola Netto, J.M., de Oliveira, G.C., and van Schooten, W. (2018). The Pharmacology of CD38/NADase: An Emerging Target in Cancer and Diseases of Aging. Trends Pharmacol Sci. *39*, 424-436. 10.1016/j.tips.2018.02.001.

17. Lee, H.C. (2001). Physiological functions of cyclic ADP-ribose and NAADP as calcium messengers. Annu Rev Pharmacol Toxicol. *41*, 317-345. 10.1146/annurev.pharmtox.41.1.317.

18. Lee, H.C., Walseth, T.F., Bratt, G.T., Hayes, R.N., and Clapper, D.L. (1989). Structural determination of a cyclic metabolite of NAD+ with intracellular

897 Ca2+-mobilizing activity. J Biol Chem. *264*, 1608-1615.
898 19. Jin, D., Liu, H.X., Hirai, H., Torashima, T., Nagai, T., Lopatina, O., Shnayder,
899 N.A., Yamada, K., Noda, M., Seike, T., et al. (2007). CD38 is critical for social
900 behaviour by regulating oxytocin secretion. Nature *446*, 41-45.
901 10.1038/nature05526.
902 20. Partida-Sánchez, S., Cockayne, D.A., Monard, S., Jacobson, E.L., Oppenheimer,
903 N., Garvy, B., Kusser, K., Goodrich, S., Howard, M., Harmsen, A., et al. (2001).
904 Cyclic ADP-ribose production by CD38 regulates intracellular calcium release,
905 extracellular calcium influx and chemotaxis in neutrophils and is required for
906 bacterial clearance in vivo. Nat Med. *7*, 1209-1216. 10.1038/nm1101-1209.
907 21. Hogan, K.A., Chini, C.C.S., and Chini, E.N. (2019). The Multi-faceted Ecto-
908 enzyme CD38: Roles in Immunomodulation, Cancer, Aging, and Metabolic
909 Diseases. Front Immunol. *10*, 1187. 10.3389/fimmu.2019.01187.
910 22. Camacho-Pereira, J., Tarragó, M.G., Chini, C.C.S., Nin, V., Escande, C., Warner,
911 G.M., Puranik, A.S., Schoon, R.A., Reid, J.M., Galina, A., and Chini, E.N.
912 (2016). CD38 Dictates Age-Related NAD Decline and Mitochondrial
913 Dysfunction through an SIRT3-Dependent Mechanism. Cell Metab. *23*, 1127-
914 1139. 10.1016/j.cmet.2016.05.006.
915 23. Tarragó, M.G., Chini, C.C.S., Kanamori, K.S., Warner, G.M., Caride, A., de
916 Oliveira, G.C., Rud, M., Samani, A., Hein, K.Z., Huang, R., et al. (2018). A
917 Potent and Specific CD38 Inhibitor Ameliorates Age-Related Metabolic
918 Dysfunction by Reversing Tissue NAD(+) Decline. Cell Metab. *27*, 1081-
919 1095.e1010. 10.1016/j.cmet.2018.03.016.
920 24. Chini, C.C.S., Peclat, T.R., Warner, G.M., Kashyap, S., Espindola-Netto, J.M.,
921 de Oliveira, G.C., Gomez, L.S., Hogan, K.A., Tarragó, M.G., Puranik, A.S., et
922 al. (2020). CD38 ecto-enzyme in immune cells is induced during aging and
923 regulates NAD(+) and NMN levels. Nat Metab. *2*, 1284-1304. 10.1038/s42255-
924 020-00298-z.
925 25. Deaglio, S., Morra, M., Mallone, R., Ausiello, C.M., Prager, E., Garbarino, G.,

Dianzani, U., Stockinger, H., and Malavasi, F. (1998). Human CD38 (ADP-ribosyl cyclase) is a counter-receptor of CD31, an Ig superfamily member. J Immunol. *160*, 395-402.

26. Deaglio, S., Aydin, S., Grand, M.M., Vaisitti, T., Bergui, L., D'Arena, G., Chiorino, G., and Malavasi, F. (2010). CD38/CD31 interactions activate genetic pathways leading to proliferation and migration in chronic lymphocytic leukemia cells. Mol Med. *16*, 87-91. 10.2119/molmed.2009.00146.

27. Piedra-Quintero, Z.L., Wilson, Z., Nava, P., and Guerau-de-Arellano, M. (2020). CD38: An Immunomodulatory Molecule in Inflammation and Autoimmunity. Front Immunol. *11*, 597959. 10.3389/fimmu.2020.597959.

28. Blacher, E., Dadali, T., Bespalko, A., Haupenthal, V.J., Grimm, M.O., Hartmann, T., Lund, F.E., Stein, R., and Levy, A. (2015). Alzheimer's disease pathology is attenuated in a CD38-deficient mouse model. Ann Neurol. *78*, 88-103. 10.1002/ana.24425.

29. Meyer, T., Shimon, D., Youssef, S., Yankovitz, G., Tessler, A., Chernobylsky, T., Gaoni-Yogev, A., Perelroizen, R., Budick-Harmelin, N., Steinman, L., and Mayo, L. (2022). NAD(+) metabolism drives astrocyte proinflammatory reprogramming in central nervous system autoimmunity. Proc Natl Acad Sci U S A. *119*, e2211310119. 10.1073/pnas.2211310119.

30. Lu, N., Dubreuil, M., Zhang, Y., Neogi, T., Rai, S.K., Ascherio, A., Hernán, M.A., and Choi, H.K. (2016). Gout and the risk of Alzheimer's disease: a population-based, BMI-matched cohort study. Ann Rheum Dis. *75*, 547-551. 10.1136/annrheumdis-2014-206917.

31. Scheepers, L., Jacobsson, L.T.H., Kern, S., Johansson, L., Dehlin, M., and Skoog, I. (2019). Urate and risk of Alzheimer's disease and vascular dementia: A population-based study. Alzheimers Dement. *15*, 754-763. 10.1016/j.jalz.2019.01.014.

32. Ames, B.N., Cathcart, R., Schwiers, E., and Hochstein, P. (1981). Uric acid provides an antioxidant defense in humans against oxidant- and radical-caused

955 aging and cancer: a hypothesis. Proc Natl Acad Sci U S A. *78*, 6858-6862.
956 10.1073/pnas.78.11.6858.
957 33. Hooper, D.C., Spitsin, S., Kean, R.B., Champion, J.M., Dickson, G.M.,
958 Chaudhry, I., and Koprowski, H. (1998). Uric acid, a natural scavenger of
959 peroxynitrite, in experimental allergic encephalomyelitis and multiple sclerosis.
960 Proc Natl Acad Sci U S A. *95*, 675-680. 10.1073/pnas.95.2.675.
961 34. Scott, G.S., Spitsin, S.V., Kean, R.B., Mikheeva, T., Koprowski, H., and Hooper,
962 D.C. (2002). Therapeutic intervention in experimental allergic
963 encephalomyelitis by administration of uric acid precursors. Proc Natl Acad Sci
964 U S A. *99*, 16303-16308. 10.1073/pnas.212645999.
965 35. Kuwabara, M., Niwa, K., Ohtahara, A., Hamada, T., Miyazaki, S., Mizuta, E.,
966 Ogino, K., and Hisatome, I. (2017). Prevalence and complications of
967 hypouricemia in a general population: A large-scale cross-sectional study in
968 Japan. PloS one *12*, e0176055. 10.1371/journal.pone.0176055.
969 36. Dalbeth, N., Gosling, A.L., Gaffo, A., and Abhishek, A. (2021). Gout. Lancet.
970 *397*, 1843-1855. 10.1016/s0140-6736(21)00569-9.
971 37. Traut, T.W. (1994). Physiological concentrations of purines and pyrimidines.
972 Mol Cell Biochem. *140*, 1-22. 10.1007/bf00928361.
973 38. Eells, J.T., and Spector, R. (1983). Purine and pyrimidine base and nucleoside
974 concentrations in human cerebrospinal fluid and plasma. Neurochem Res. *8*,
975 1451-1457. 10.1007/bf00965000.
976 39. Dudzinska, W., Lubkowska, A., Dolegowska, B., Safranow, K., and
977 Jakubowska, K. (2010). Adenine, guanine and pyridine nucleotides in blood
978 during physical exercise and restitution in healthy subjects. Eur J Appl Physiol.
979 *110*, 1155-1162. 10.1007/s00421-010-1611-7.
980 40. Fridovich, I. (1965). THE COMPETITIVE INHIBITION OF URICASE BY
981 OXONATE AND BY RELATED DERIVATIVES OF S-TRIAZINES. J Biol
982 Chem. *240*, 2491-2494.
983 41. Mills, K.F., Yoshida, S., Stein, L.R., Grozio, A., Kubota, S., Sasaki, Y., Redpath,

984 P., Migaud, M.E., Apte, R.S., Uchida, K., et al. (2016). Long-Term
985 Administration of Nicotinamide Mononucleotide Mitigates Age-Associated
986 Physiological Decline in Mice. Cell Metab. *24*, 795-806.
987 10.1016/j.cmet.2016.09.013.
988 42. Minhas, P.S., Liu, L., Moon, P.K., Joshi, A.U., Dove, C., Mhatre, S., Contrepois,
989 K., Wang, Q., Lee, B.A., Coronado, M., et al. (2019). Macrophage de novo
990 NAD(+) synthesis specifies immune function in aging and inflammation. Nat
991 Immunol. *20*, 50-63. 10.1038/s41590-018-0255-3.
992 43. Misawa, T., Takahama, M., Kozaki, T., Lee, H., Zou, J., Saitoh, T., and Akira,
993 S. (2013). Microtubule-driven spatial arrangement of mitochondria promotes
994 activation of the NLRP3 inflammasome. Nat Immunol. *14*, 454-460.
995 10.1038/ni.2550.
996 44. Murakami, T., Ockinger, J., Yu, J., Byles, V., McColl, A., Hofer, A.M., and
997 Horng, T. (2012). Critical role for calcium mobilization in activation of the
998 NLRP3 inflammasome. Proc Natl Acad Sci U S A. *109*, 11282-11287.
999 10.1073/pnas.1117765109.
1000 45. Zeidler, J.D., Kashyap, S., Hogan, K.A., and Chini, E.N. (2022). Implications
1001 of the NADase CD38 in COVID pathophysiology. Physiol Rev. *102*, 339-341.
1002 10.1152/physrev.00007.2021.
1003 46. Joosten, L.A.B., Crişan, T.O., Bjornstad, P., and Johnson, R.J. (2020).
1004 Asymptomatic hyperuricaemia: a silent activator of the innate immune system.
1005 Nat Rev Rheumatol. *16*, 75-86. 10.1038/s41584-019-0334-3.
1006 47. Lowell, C.A. (2022). Hyperuricemia reduces neutrophil function. Blood *139*,
1007 3354-3356. 10.1182/blood.2022016275.
1008 48. Gomez, G., and Sitkovsky, M.V. (2003). Differential requirement for A2a and
1009 A3 adenosine receptors for the protective effect of inosine in vivo. Blood *102*,
1010 4472-4478. 10.1182/blood-2002-11-3624.
1011 49. Álvarez-Lario, B., and Macarrón-Vicente, J. (2010). Uric acid and evolution.
1012 Rheumatology (Oxford). *49*, 2010-2015. 10.1093/rheumatology/keq204.

1013 50. Chang, B.S. (2014). Ancient insights into uric acid metabolism in primates. Proc
1014 Natl Acad Sci U S A. *111*, 3657-3658. 10.1073/pnas.1401037111.
1015 51. Rajman, L., Chwalek, K., and Sinclair, D.A. (2018). Therapeutic Potential of
1016 NAD-Boosting Molecules: The In Vivo Evidence. Cell Metab. *27*, 529-547.
1017 10.1016/j.cmet.2018.02.011.
1018 52. Peclat, T.R., Shi, B., Varga, J., and Chini, E.N. (2020). The NADase enzyme
1019 CD38: an emerging pharmacological target for systemic sclerosis, systemic
1020 lupus erythematosus and rheumatoid arthritis. Curr Opin Rheumatol. *32*, 488-
1021 496. 10.1097/bor.0000000000000737.
1022 53. Becker, M.A., Schumacher, H.R., Jr., Wortmann, R.L., MacDonald, P.A.,
1023 Eustace, D., Palo, W.A., Streit, J., and Joseph-Ridge, N. (2005). Febuxostat
1024 compared with allopurinol in patients with hyperuricemia and gout. N Engl J
1025 Med. *353*, 2450-2461. 10.1056/NEJMoa050373.
1026 54. Hooftman, A., Angiari, S., Hester, S., Corcoran, S.E., Runtsch, M.C., Ling, C.,
1027 Ruzek, M.C., Slivka, P.F., McGettrick, A.F., Banahan, K., et al. (2020). The
1028 Immunomodulatory Metabolite Itaconate Modifies NLRP3 and Inhibits
1029 Inflammasome Activation. Cell Metab. *32*, 468-478.e467.
1030 10.1016/j.cmet.2020.07.016.
1031 55. Ives, A., Nomura, J., Martinon, F., Roger, T., LeRoy, D., Miner, J.N., Simon, G.,
1032 Busso, N., and So, A. (2015). Xanthine oxidoreductase regulates macrophage
1033 IL1β secretion upon NLRP3 inflammasome activation. Nat Commun. *6*, 6555.
1034 10.1038/ncomms7555.
1035 56. Wen, S., Arakawa, H., and Tamai, I. (2021). CD38 activation by monosodium
1036 urate crystals contributes to inflammatory responses in human and murine
1037 macrophages. Biochem Biophys Res Commun. *581*, 6-11.
1038 10.1016/j.bbrc.2021.10.010.
1039 57. FitzGerald, J.D., Dalbeth, N., Mikuls, T., Brignardello-Petersen, R., Guyatt, G.,
1040 Abeles, A.M., Gelber, A.C., Harrold, L.R., Khanna, D., King, C., et al. (2020).
1041 2020 American College of Rheumatology Guideline for the Management of

1042 Gout. Arthritis Rheumatol. *72*, 879-895. 10.1002/art.41247.
1043 58. Yamanaka, H., Tamaki, S., Ide, Y., Kim, H., Inoue, K., Sugimoto, M., Hidaka,
1044 Y., Taniguchi, A., Fujimori, S., and Yamamoto, T. (2018). Stepwise dose
1045 increase of febuxostat is comparable with colchicine prophylaxis for the
1046 prevention of gout flares during the initial phase of urate-lowering therapy:
1047 results from FORTUNE-1, a prospective, multicentre randomised study. Ann
1048 Rheum Dis. *77*, 270-276. 10.1136/annrheumdis-2017-211574.
1049 59. Ichinose, W., Cherepanov, S.M., Shabalova, A.A., Yokoyama, S., Yuhi, T.,
1050 Yamaguchi, H., Watanabe, A., Yamamoto, Y., Okamoto, H., Horike, S., et al.
1051 (2019). Development of a Highly Potent Analogue and a Long-Acting Analogue
1052 of Oxytocin for the Treatment of Social Impairment-Like Behaviors. J Med
1053 Chem. *62*, 3297-3310. 10.1021/acs.jmedchem.8b01691.
1054 60. de Oliveira, G.C., Kanamori, K.S., Auxiliadora-Martins, M., Chini, C.C.S., and
1055 Chini, E.N. (2018). Measuring CD38 Hydrolase and Cyclase Activities: 1,N(6)-
1056 Ethenonicotinamide Adenine Dinucleotide (ε-NAD) and Nicotinamide Guanine
1057 Dinucleotide (NGD) Fluorescence-based Methods. Bio Protoc. *8*.
1058 10.21769/BioProtoc.2938.
1059 61. Higashida, H., Egorova, A., Higashida, C., Zhong, Z.G., Yokoyama, S., Noda,
1060 M., and Zhang, J.S. (1999). Sympathetic potentiation of cyclic ADP-ribose
1061 formation in rat cardiac myocytes. J Biol Chem. *274*, 33348-33354.
1062 10.1074/jbc.274.47.33348.
1063